BREATH: Heat Maps Assisting the Detection of Abnormal Lung Regions in CT Scans

Mirela T. Cazzolato*, Lucas C. Scabora*, Alceu F. Costa*, Marcos R. Nesso-Jr*, Luis F. Milano-Oliveira†, Daniel S. Kaster†, Caetano Traina-Jr*, Agma J. M. Traina*
*Institute of Mathematics and Computer Science - University of São Paulo, USP, São Carlos, Brazil
†Department of Computer Science - University of Londrina, UEL, Londrina, Brazil
mirelac@usp.br, lucascsb@usp.br, alceufc@icmc.usp.br, marcosnesso@usp.br, luismilanooliveira@gmail.com, dskaster@uel.br, caetano@icmc.usp.br, agma@icmc.usp.br

***Abstract*—Computed Tomography (CT) scans are often employed to diagnose lung diseases, as abnormal tissue regions may indicate whether proper treatment is required. However, detecting specific regions containing abnormalities in a CT scan demands time and effort of specialists. Moreover, different parts of a single lung image may present both normal and abnormal characteristics, what makes inaccurate the classification of a single lung as healthy (normal) or not. In this paper we propose the BREATH method, capable of detecting abnormalities in lung tissue regions, highlighting them by means of a heat map visualization. The method starts by segmenting lung tissues using a superpixel-based approach, followed by the training of a statistical model to represent normal tissues and, finally, the generation of a heat map showing abnormal regions that require attention from the physicians. We validated our statistical model using a dataset with 246 lung CT scans, where 40 are healthy and the remaining present varying diseases. Experimental results show that BREATH is accurate for lung segmentation with F-Measure of up to 0.99. The statistical modeling of healthy and abnormal lung regions has shown almost no overlap, and the detection of superpixels containing abnormalities presented precision values higher than 86%, for all values of recall. Finally, the heat map representation of BREATH for the abnormal detection has been shown to be an intuitive method to assist physicians during the diagnosis.**

***Keywords*-Lung diseases; CT scans; heat map; statistical modeling; classification; CBIR; texture; superpixel.**

I. Introduction

Automated image classification and retrieval have applications in many scenarios [1], such as social media, emergency situations and clinical environments. Specifically in clinical environments, imaging exams are constantly generated in increasing amount and resolution. Due to the use of digital images as a part of the diagnosis process, an automatic classification approach can help the clinical decision-making process [2]. Content-Based Image Retrieval (CBIR) applications assist physicians to analyze large amounts of images, finding similar exams and helping them to provide fast and accurate diagnosis, mainly based on historical and already diagnosed exams. In this work we are interested in supporting the detection of diseases in lung Computed Tomography (CT) scans. Lung diseases can be diagnosed by detecting abnormal patterns in CT scans, considering visual clues such as gray-level distribution and texture patterns.

One of the major challenges in the retrieval or classification task is that the definition of similarity depends on the application. Existing works have shown several issues regarding the segmentation of lung regions and detection of which abnormality occurs in the image [3][4]. There is no consensus regarding which features are the most suitable for the lung image representation [5] or which is the best classifier to use [6]. Also, the detection approach must consider only regions of the lungs in the pattern recognition process, which requires a preprocessing step to delimit the lung tissue regions from the CT images, as depicted in Figure 1. Finally, radiologists usually prefer applications that preprocess the images to be analyzed to highlight those presenting patterns that demand cautious analysis than fully automated diagnosing methods.

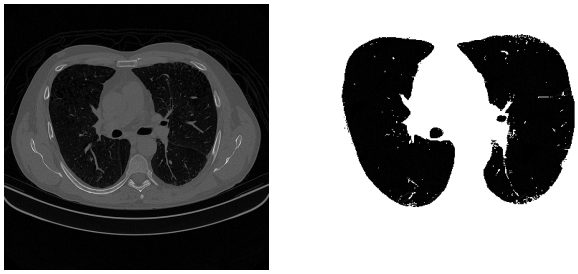

(a) (b)

Figure 1. Example of a lung CT scan. (a) The image can be divided into three main parts: lung tissue (the two internal regions, presenting darker color and texture patterns); body cavity (light gray); and the outside (external part). (b) The segmented lung regions.

In this work we are interested in solving the following problem: *given a lung CT image, how to* ***model the healthy lung tissue behavior*** *and compose a* ***heat map visualization*** *of lung regions, according to their* ***likelihood of being abnormal****?* To address this problem, we propose a new approach able to segment lung regions of a CT scan by dividing the image into superpixels (*i.e.* a set of pixels that present homogeneous behavior). The superpixel regions identified as lung tissue are then classified by a supervised model,

in order to detect the presence or absence of abnormalities based on the behavior analysis of previously known healthy regions. Notice that a lung may present regions with different patterns, such as healthy and emphysema regions in a single CT image. Therefore, our approach performs a "continuous classification" of lung regions, according to a score that indicates the deviation from an average normal tissue, and provides a visualization that helps the radiologist to focus on abnormal regions. The contributions of our proposal compose the method BREATH, which is able to:

1) automatically segment lung CT scans using superpixels, in order to obtain only lung tissue regions;
2) model the behavior of a healthy lung tissue, making it possible to determine the likelihood score of a lung superpixel to contain an abnormality; and
3) assist physicians with a visual representation of the abnormalities found in the lung CT image, highlighting the score of each region with a heat map.

The remaining of this paper is organized as follows. In Section II we briefly present the background concepts related to our proposal, and in Section III we give an overall description of the related work, regarding lung disease detection in images. In Section IV we describe our proposal. We provide an experimental analysis and discussion of our proposal in Section V. Finally, in Section VI we present the final conclusions of this work.

II. Background

Formally, let I be an image, such that $I = \{p_i | 0 \leq i \leq n\}$, where p_i is a pixel, n is the number of pixels in I, and $0 \leq p_i \leq R-1$, where R is the number of levels the image was quantized. A superpixel is a subset $S \subseteq I$ defined as $S = \{p_j | 0 < j < m\}$, where m is the number of pixels inside a superpixel and $m < n$. The set of superpixels of an image is a partition on I and is denoted by $\mathcal{S}$.

A Feature Extraction Method (FEM) $\mathcal{E}$, or simply a **extractor**, is a non-bijective function such that $\mathcal{E} : S \rightarrow \mathbb{R}^d$. In this scenario, given a superpixel $S \in \mathcal{S}$ of I, $\mathcal{E}$ maps S to a $d-$dimensional feature vector. Let $\mathcal{V}_\mathcal{T}$ be a set of feature vectors extracted from superpixel regions of the set of training images, and $\mathcal{L}$ be the set of (external) available labels. Each training feature vector $\mathbf{v}_t \in \mathcal{V}_\mathcal{T}$ has a label assigned by an expert. Let $\mathcal{V}$ be the set of feature vectors that represents the superpixels of an image to be segmented. A supervised classifier $\mathcal{C}$ uses the set $\mathcal{V}_\mathcal{T}$ to train a model that will be used to predict the label $l_i \in \mathcal{L}$ for each region of $v \in \mathcal{V}$, such that $v \in \mathbb{R}^d$.

In our proposal, new regions classified by $\mathcal{C}$ are **superpixels**, extracted from lung images. The application of a classifier $\mathcal{C}$ over $\mathcal{S}$ allows us to compose the segmented images, considering the set of available labels. Details of this segmentation step are given in Section IV. There is a large amount of strategies to segment an image into superpixel regions in the literature. For our proposal we employed the Simple Linear Iterative Clustering (SLIC) approach [7]. SLIC is a fast and memory efficient algorithm, suitable for superpixel generation, that uses an improved version of k-means and presents accurate results in comparison with the state-of-the art superpixel approaches [7][8].

III. Related Work

The issue of classifying pulmonary patterns based on visual features has been thoroughly studied for several years. In [9], a set of 18 textural features was extracted from image blocks in order to recognize pulmonary patterns through an SVM classifier. By combining different block sizes through a Bayesian approach, the authors achieved a high accuracy. The work of [10] considered the usage of wavelet frames and gray-level histograms as textural features for high-resolution lung CT scans with Interstitial Lung Disease (ILD). The extracted features were used as input to a kNN classifier, which was able to reach an accuracy of 92.5% in a multiclass scenario. Despite its good results, this method requires a set of ROIs previously annotated by a specialist.

In [4], the authors explore the fact that many lung tissue patterns are not entirely captured by intensity-only segmentation. They proposed an alternative method based on graph search, leveraged by a cost function combining intensity with gradient, boundary smoothness, and rib information, being capable of automatically segment lung CT images for detecting ILD. This problem was also addressed in [11], where the lung region is fully separated from the background CT slice through the usage of the active contour with distance regularized level. The technique proposed by [5] uses Completed LBP features and a SVM classifier for ILD recognition in CT scans that had their ROI pre-annotated by a specialist. By using this approach, the authors reached levels of accuracy that are competitive to those of methods that do use CT scans already segmented and classified as lung and non-lung. However, the non-homogeneous nature of some pulmonary patterns proved to be a problem to texture-only features, resulting in a degraded performance.

Finally, the issue of classifier fusion was addressed in [6] for detecting common CT imaging lung diseases, using confusion matrices and classification confidence of five well-known classifiers. The proposed method was able to improve the overall accuracy in up to 12.3%.

The aforementioned works have as their main focus the automatic detection of a set of diseases in lung images. However, they either employ segmentation techniques too inflexible when compared to a superpixel based approach or focus on performing an automatic classification of the images. We propose to use superpixel based segmentation for discriminate lung from non-lung regions, alongside with a statistical model to characterize normal tissue and detect abnormal lung tissue based on textural and color features for ILD detection, quantifying its deviation from the normal. Our primary goal is to provide a visualization that highlights

regions of interest using a continuous score in order to assist specialists in the diagnosing process and support training of technicians and residents.

IV. The BREATH Method: Detecting Healthy and Abnormal Tissues in Lung CT Scans

In this section we propose BREATH, an automatic detector of abnormalities in lung regions of CT scans. BREATH is composed of three main steps, as depicted in Figure 2:

a) segmentation of lung regions of lung CT scans;
b) training of a statistical model based on the visual properties of healthy lung tissues;
c) automatic detection of lung abnormalities, providing a heat map visualization of the result.

A. Segmentation of Lung Regions from CT Images

As we can see in Figure 1, a CT image is composed not only of regions with lung tissue, but also with other structures. Given a lung CT image, BREATH starts by generating a set of m superpixels, as shown in Figure 2(a). Then, for each superpixel s_i a Feature Extraction Method (FEM) $\mathcal{E}$ is employed to obtain the corresponding feature vector $\mathbf{v}_i$. We used the Local Binary Pattern (LBP) extractor, as it allows us to compare regions of lung tissue from different CT scans that could have underwent different settings for contrast enhancing. The input to the LBP extractor is the minimum boundary rectangle (MBR) of each superpixel. Since not all pixels from the MBR are part of the superpixel, we built a binary mask that takes the value 1 for pixels belonging to the superpixel and 0 otherwise. When computing the histogram of binary patterns, LBP was adapted to ignore pixels and their neighbors that have value 0 in the binary mask.

After the feature extraction, BREATH employs a classifier to assign to each superpixel a value from the set of labels $\mathcal{L}_D = \{lung, body, other\}$, which represent the three main patterns depicted in a lung CT. Since we are interested in the detection of abnormalities occurring in lung tissues, the output of BREATH's segmentation step is an image composed only of superpixels classified as *lung*.

B. Characterization of Healthy Lung Tissue

Are there visual patterns in CT scans that can be used to discriminate between healthy and abnormal lung tissue? In this section, we show:

1) how BREATH uses a statistical model to characterize the visual properties of healthy lung tissues;
2) that the majority of the superpixels depicting abnormalities deviate from this statistical model.

BREATH's characterization of healthy lung tissue starts with the projection of the superpixels' visual features into a lower dimensional feature space using Principal Component Analysis (PCA), as shown in Figure 2(b). The visual features used to represent the superpixels in this step of our method were previously extracted in the segmentation step of BREATH (Section IV-A).

Figure 3(a) shows a two-dimensional PCA projection of healthy superpixels in the feature space. Each dot corresponds to a projected superpixel feature vector. We observe that the superpixels form a single cluster of points that we model as a multivariate normal distribution.

To train the model, we estimate the parameters of a multivariate normal distribution to describe the PCA-projected visual features of healthy lung tissue. Given a PCA-projected feature vector $\mathbf{v} = (v_1, v_2, \cdots, v_n)$ extracted from a superpixel, the Probability Distribution Function (PDF) $f(\mathbf{v})$ of the multivariate normal distribution returns the likelihood that $\mathbf{v}$ describes a healthy lung tissue:

$$f(\mathbf{v}) = \frac{\exp\left(\frac{1}{2}(\mathbf{v}-\boldsymbol{\mu})^T\boldsymbol{\Sigma}^{-1}(\mathbf{v}-\boldsymbol{\mu})\right)}{\sqrt{|2\pi\boldsymbol{\Sigma}|}} \quad (1)$$

where $\boldsymbol{\mu}$ and $\boldsymbol{\Sigma}$ are respectively the computed mean from the feature vector and the covariance matrix. To estimate $\boldsymbol{\mu}$ and $\boldsymbol{\Sigma}$ we use the Maximum Likelihood Estimation (MLE) using only feature vectors from superpixels depicting a healthy tissue.

The black lines in Figure 3(a) correspond to the contour plot of the fitted multivariate normal distribution. This distribution accurately describes the feature vectors distribution of superpixels representing healthy regions of the images. Figure 3(b), shows the PCA projection of unlabeled superpixels depicting both healthy lung tissues and abnormalities. Notice that many projected feature vectors deviate from the normal distribution observed for healthy superpixels. This simple, but accurate model leads to an important corner stone for the next step of BREATH.

C. Detection of Lung Abnormalities

As we discussed in the previous section, a PCA-projected multivariate normal distribution provides an accurate description of the distribution of healthy feature vectors. As a result, given an unlabeled feature vector $\mathbf{v}'$, the value of the PDF $f(\mathbf{v}')$ provides an estimate of the likelihood that $\mathbf{v}'$ was extracted from a CT region depicting a healthy lung tissue, as presented in Figure 2(c). Conversely, a small value of $f(\mathbf{v})$ indicates that the feature vector $\mathbf{v}'$ was likely extracted from a CT region depicting an abnormality.

After computing $f(\mathbf{v})$ for each superpixel, BREATH generates an output heat map representation of the lungs, where: the highest value of $f(\mathbf{v})$ is drawn with the darkest color (black), thus most likely representing healthy tissues; and the smallest values of $f(\mathbf{v})$ are depicted with light colors (in this case, orange), and represents the superpixels most likely extracted from CT regions depicting abnormality. This heat map can be presented alongside the original lung CT scan, in order to assist the physicians in the diagnosis process,

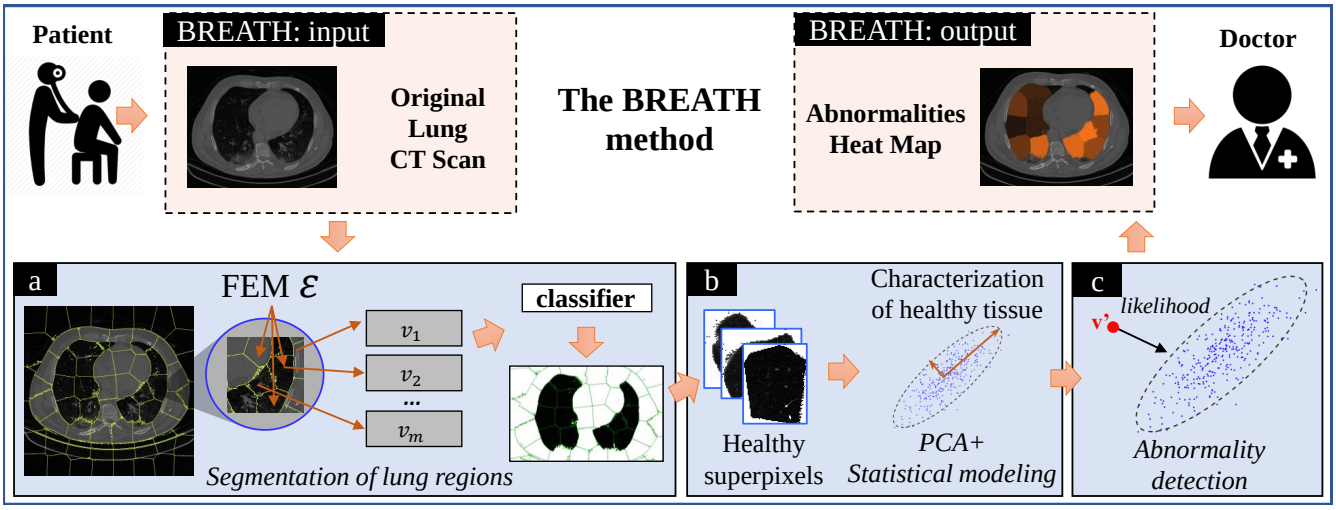

Figure 2. The BREATH method to detect lung abnormalities: given a lung CT scan, (a) BREATH segments the image using supepixel classification, generating an image with only lung tissues. (b) The characterization of healthy lung tissue is done using principal component analysis and statistical modeling. The constructed model is used (c) to determine the likelihood of a superpixel to contain abnormality. BREATH outputs a heat map representation of the lung, with the CT regions depicting abnormalities with lighter colors, and healthy CT regions with darker colors.

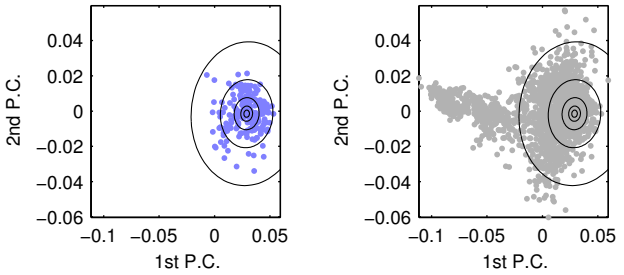

(a) Healthy Superpixels (b) All Superpixels

Figure 3. Results of the Statistical Model: PCA projection of superpixel feature vectors. (a) Superpixels depicting only healthy lung tissue (blue dots) whose distribution can be fitted by a multivariate distribution (black lines indicate the contour plot of the distribution PDF). (b) Projection of unlabeled superpixels features. Note that the distribution deviates from the normal distribution.

by highlighting the regions of the lung that should be more carefully observed.

V. Experimental Analysis and Discussion

In this section we present an experimental analysis of BREATH, describing the employed dataset and the validation of each step of the proposed method.

A. Dataset

For the experimental analysis of our proposal we used a dataset of lung CT scans, acquired in the Clinical Hospital of the Ribeirão Preto Medical School, in Brazil. Each CT scan has 512×512 pixels, with a slice thickness of 1 millimeter. The dataset is composed of 246 images, where 40 of them correspond to CT scans of healthy patients, while the remaining presents at least one of the following abnormalities: consolidation, emphysema, thickening, honeycombing and ground glass. Table I shows the dataset class distribution.

Table I
Dataset overview.

Label	# Images
Healthy	40
Consolidation	40
Emphysema	44
Thickening	42
Honeycombing	39
Ground Glass	41

B. Segmenting Lung Regions

For the lung segmentation step of BREATH, our objective was to divide the superpixels of the CT scans in three sets: *lung*, *body* and *other*. The superpixels were manually labeled as: lung tissue (1,742), body cavity (2,031) and other (2,356). Then, we extracted the feature vectors of each set using two extractors (Color Histogram and LBP) and tested the following classifiers: k-Nearest Neighbor (kNN), Random Forest (RF), Multilayer Perceptron (MLP) and Support Vector Machine (SVM). The results obtained after performing a ten-fold cross-validation are presented in Table II. As we can observe, although using off-the-shelf extractors, the classifiers were able to accurately differentiate the regions of lung CT scans, presenting an F-Measure of up to 0.99 using color histogram features and up to 0.96 using LBP features.

Table II
CLASSIFICATION RESULTS OF THE LUNG SEGMENTATION STEP OF BREATH: THE CLASSIFIERS WERE ABLE TO ACCURATELY DIFFERENTIATE THE REGIONS OF LUNG CT SCANS.

FEM	# dimensions	F-Measure			
		1NN	RF	MLP	SVM
Histogram	32	0.989	**0.993**	0.988	0.948
	64	0.992	**0.994**	0.986	0.954
	128	**0.994**	**0.994**	0.984	0.956
	256	**0.992**	**0.992**	0.973	0.95
LBP	16	0.908	**0.939**	0.331	0.859
	256	0.894	**0.965**	0.345	0.66

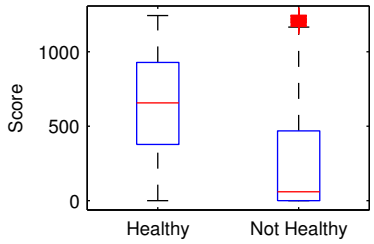

Figure 4. BREATH discriminates between healthy and abnormal lung tissue. The box-plot compares the distribution of likelihood scores returned by BREATH's statistical model for superpixels depicting healthy and not-healthy lung tissue.

C. Abnormality Detection: Quantitative Results

In this section we evaluate how well BREATH is able to detect abnormalities taking advantage of superpixels depicting the lung tissue. Although we have the label of every CT slice for evaluation purposes (e.g., healthy or consolidation), we do not have the label for the individual superpixels. For instance, a CT slice labeled as honeycombing could also contain regions of healthy lung tissue.

To validate our method, we employed several datasets, and will show the results considering a representative labeled dataset of regions of interest (ROIs) of lung tissue [1]. The dataset has 3,258 ROIs, of 64×64 pixels, labeled by an expert using either a healthy lung tissue or one of the following abnormalities: consolidation, emphysema, thickening, honeycombing and ground glass. We extracted the LBP features (as described in Section IV-A) from each ROI, trained a k-Nearest Neighbor classifier with $k = 3$ and used the city-block distance. We performed a ten-fold cross-validation on the ROI data and the classifier was *highly accurate*, obtaining an accuracy of $97.8\% \pm 0.7\%$. We used this classifier to label the superpixels as either positive (presenting abnormalities) or negative (healthy tissue). The labels assigned by the classifier were employed as the ground truth for the experiments described following in this section.

We start by analyzing how well BREATH's statistical model, presented in Section IV-B, is able to describe healthy superpixel visual features. Figure 4 shows a box-plot comparing the likelihood score returned by the BREATH's statistical model of superpixels classified as healthy (normal) or not-healthy (abnormal). The scores assigned by the statistical model were able to clearly separate the majority of the superpixels. More specifically, the interquartile range (indicated by the blue boxes) of healthy superpixels has upper scores, and with almost no overlap with the interquartile range of the superpixels presenting abnormalities.

We also evaluated how well BREATH is able to detect abnormal lung tissues. Figure 5 shows the precision vs. recall (sensitivity) curve for the task of detecting superpixels depicting abnormalities. To classify a superpixel as healthy or not, we used a BREATH's likelihood score. The precision vs. recall curve was built varying the decision threshold with respect to the likelihood score. In a precision vs. recall curve, the best performance is indicated by the curve closest to the top for different values of recall. BREATH was able to obtain a precision higher than 86% for all values of recall, presenting an average accuracy of 95%.

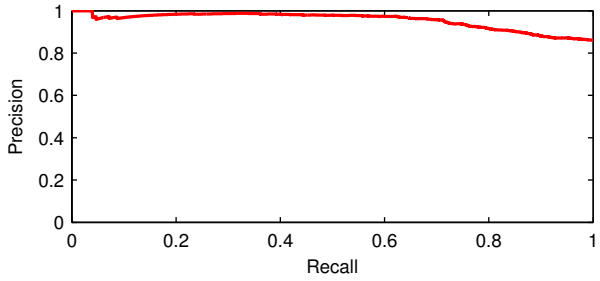

Figure 5. Precision vs. recall curve for the task of detecting superpixels depicting abnormalities. BREATH was highly accurate, as indicated by the curve close to top (i.e. precision close to 1) for every recall (sensitivity).

D. Abnormality Detection: Qualitative Results

With the characterization of healthy and abnormal lung tissues, BREATH composes an output image using a heat map representation, as shown in Figure 6. The statistical model used to classify lung regions outputs a continuous value, corresponding to the likelihood of each superpixel to be a healthy tissue. This allows BREATH to use lighter colors (near orange) to represent regions that are likely to contain abnormality, and darker colors (near black) to represent healthy lung tissue regions.

By analyzing the output images depicted in Figure 6(b) and (d), it is possible to observe that the heat map representation highlights the superpixel regions presenting different texture patterns using different color tones, as expected. Also, by looking at the resulting heat map image, the physician's attention is addressed to analyze more carefully the regions most likely to have an abnormality (i.e. that

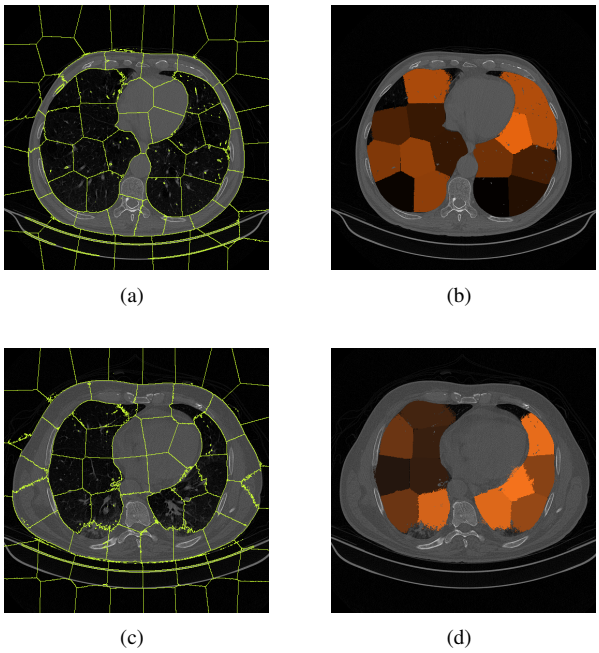

Figure 6. BREATH outputs a heat map representation based on the probability of each superpixel to contain an abnormality. (a) and (c) shows the lung CT scan with the superpixels' contour, and (b) and (d) depicts the generated heat map of BREATH. Lighter colors (orange) represent the lung regions with the highest probability of containing an abnormality. Thus, the darker colors represent regions with lung tissue similar to the healthy ones.

presents a different visual pattern when compared to healthy lung tissues).

VI. Conclusion

In this work we dealt with the problem of abnormality detection in lung CT scans, with the goal of assisting physicians during the diagnoses process. We proposed the BREATH method, that segments lung regions in CT scans based on superpixel classification. Experimental results has shown that BREATH was able to differentiate lung tissues from the rest of the image with a F-Measure up to 0.99. The second goal of this work was to characterize lung tissues according to their visual features. To address this goal, our method first describes the healthy lung tissues using a statistical modeling process, taking into account that the visual properties of abnormalities deviate from the healthy statistical model. The experimental results indicate that the scores assigned to each lung tissue region by the statistical model were able to clearly separate the majority of superpixels. After this characterization, the model is used to compute the likelihood of a lung superpixel to contain an abnormality, by means of the maximum likelihood estimation. The method presented steady precision values, higher than 86% for all values of recall. Finally, BREATH provides a heat map representation of the likelihood scores, composing an output image with the regions being highlighted according to the probability of a region to contain an abnormality. This representation can be used to assist the physicians during the diagnosis process, helping to identify the lung regions that most likely contain an abnormality.

References

[1] A. F. Costa, G. Humpire-Mamani, and A. J. M. Traina, "An efficient algorithm for fractal analysis of textures," in *25th SIBGRAPI*, ser. SIBGRAPI '12. Washington, DC, USA: IEEE Computer Society, 2012, pp. 39–46.

[2] C. Burak Akgül, D. L. Rubin, S. Napel, C. F. Beaulieu, H. Greenspan, and B. Acar, "Content-based image retrieval in radiology: Current status and future directions," *Journal of Digital Imaging*, vol. 24, no. 2, pp. 208–222, 2011.

[3] F. Zhang, Y. Song, W. Cai, Y. Zhou, S. Shan, and D. Feng, "Context curves for classification of lung nodule images," in *DICTA 2013*, Nov 2013, pp. 1–7.

[4] P. Hua, Q. Song, M. Sonka, E. A. Hoffman, and J. M. Reinhardt, "Segmentation of pathological and diseased lung tissue in ct images using a graph-search algorithm," in *8th ISBI*, March 2011, pp. 2072–2075.

[5] L. D. Bagesteiro, L. F. Oliveira, and D. Weingaertner, "Block-wise classification of lung patterns in unsegmented ct images," in *28th CBMS*, June 2015, pp. 177–182.

[6] L. Ma, X. Liu, L. Song, C. Zhou, X. Zhao, and Y. Zhao, "A new classifier fusion method based on historical and on-line classification reliability for recognizing common CT imaging signs of lung diseases," *Computerized Medical Imaging and Graphics*, vol. 40, pp. 39 – 48, 2015.

[7] R. Achanta, A. Shaji, K. Smith, A. Lucchi, P. Fua, and S. Süsstrunk, "Slic superpixels compared to state-of-the-art superpixel methods," *IEEE Transactions on Pattern Analysis and Machine Intelligence*, vol. 34, no. 11, pp. 2274–2282, Nov 2012.

[8] M. T. Cazzolato, M. V. N. Bedo, A. F. Costa, J. A. de Souza, C. T. Jr., J. F. R. Jr., and A. J. M. Traina, "Unveiling smoke in social images with the smokeblock approach," in *31st SAC*, Pisa, Italy, April 2016, pp. 49–54.

[9] J. Malone, J. M. Rossiter, S. Prabhu, and P. Goddard, "Identification of disease in ct of the lung using texture-based image analysis," in *38th ASILOMAR*, vol. 2. IEEE, 2004, pp. 1620–1624.

[10] A. Depeursinge, D. Sage, A. Hidki, A. Platon, P.-A. Poletti, M. Unser, and H. Muller, "Lung tissue classification using wavelet frames," in *29th EMBS*. IEEE, 2007, pp. 6259–6262.

[11] M. D. Raj and C. H. Sulochana, "An efficient lung segmentation approach for interstitial lung disease," in *16th ICCPCT*. IEEE, 2014, pp. 1211–1216.